INL/JOU-22-68425-Revision-0

High temperature annealing of irradiated nuclear grade graphite

June 2023

Douglas John Stevens, William E Windes, David T Rohrbaugh, David L Cottle

Changing the World's Energy Future

INL is a U.S. Department of Energy National Laboratory operated by Battelle Energy Alliance, LLC

INL/JOU-22-68425-Revision-0

High temperature annealing of irradiated nuclear grade graphite

Douglas John Stevens, William E Windes, David T Rohrbaugh, David L Cottle

June 2023

Idaho National Laboratory
Idaho Falls, Idaho 83415

http://www.inl.gov

Prepared for the
U.S. Department of Energy
Under DOE Idaho Operations Office
Contract DE-AC07-05ID14517

Version of Record: https://www.sciencedirect.com/science/article/pii/S0022311523001472
Manuscript_ac7c2c7e4871ae0be6b89828179f2a59

High Temperature Annealing of Irradiated Nuclear Grade Graphite

Steve Johns*, William E. Windes, David T. Rohrbaugh, and David L. Cottle
Idaho National Engineering Laboratory
PO Box 1625, Idaho Falls, ID 83415, USA

Abstract

Previous work has shown that the material properties of nuclear grade graphite are substantially affected by the atomic and microstructural changes that occur during neutron-irradiation. The parameters that play a role in these changes are irradiation dose, temperature, graphite composition and the initial microstructure of the graphite. Understanding the details of how these material changes occur and exactly what the changes consists of will enable the prediction of the material property changes as a function of these variables. Other work has shown these atomic level and microstructural changes can be healed or annealed out by raising the irradiated graphite above its irradiation temperature. In this work, experiments were carried out to investigate how the properties of irradiated graphite recover when heated. By showing property recovery as a function of annealing temperature or energy, insight is provided into the type of damage that occurred during neutron-irradiation. The data presented here shows recovery of thermal diffusivity, coefficient of thermal expansion, Young's modulus and electrical resistivity between annealing temperatures of 500°C and 2380°C. Graphite grades NBG-18, IG-110 and PCEA are considered that were both stressed and unstressed during irradiation.

*Corresponding author. Tel: 208 526-7017. E-mail: Steven.johns@inl.gov (Steve Johns)

1. Introduction

Graphite has a long history as a moderator material for nuclear reactors, including the first reactor to achieve criticality, Chicago Pile 1 in 1942. Since that time nuclear graphite has remained a candidate material for reactors designs including but not limited to, the 28 Magnox and 14 Advanced Gas-cooled Reactor (AGR) concepts built in the United Kingdom, the RBMK designs of the Soviet Union, China's HTR-10 which is in-service, the United States research reactor TREAT, and the high-temperature gas-cooled (HTGR) Fort St. Vrain. Additionally, the Generation IV International forum (GIF) has identified two of six reactor concepts for research and development to be graphite moderator reactors; specifically, the Molten Salt Reactor (MSR) and the Very High-temperature Reactor (VHTR). For graphite moderated reactors, the limiting factor for in-service use is the graphite itself. To improve the longevity of future reactor concepts, a comprehensive understanding of the irradiation induced damage mechanisms is needed.

When graphite is irradiated with fast neutrons various lattice defects are produced. These defects range from simple single vacancies and interstitials to more complex vacancy groups which can cause distortion to the graphite basal planes [1]. Proposed models of this damage vary from relatively simple Frenkel pair vacancy-interstitial explanations to more complex $sp^2 – sp^3$ bonding transitions [1–3] As the damage accumulates, the evolution of point defects has been proposed to result in many possible larger three-dimensional defects. Koike's [4] room temperature electron-irradiation provided evidence to support fragmentation of basal planes due to interstitial clusters; however, this proposed theory was contradicted by Muto [5] who proposed room temperature electron-irradiation to result in homogenous swelling of the lattice spacing and not fragmentation. Others show room temperature irradiations to result in additional basal plane formation via dislocation climb [6]; however, damage mechanisms in nuclear graphite are temperature dependent, and damage mechanisms from irradiations conducted above 250°C differ significantly from that of room temperature irradiations [7,8] Elevated temperature irradiations (neutron, electrons, and ions) show possible mechanisms ranging from densification of porosity, 'kink bands', to the formation of more exotic fullerene-like structures [9–14]. In addition to experimental results, computational modelling is as equally vast in diversity of proposed mechanisms, including but not limited to: cross-linking vacancy species, prismatic defects, ripplocations, to the more unusual 'buckle, ruck and tuck' model [15–20]. To date a definitive model does not exist and it is

likely that only a combination of theories will explain the changes in physical properties observed in graphite following irradiation [19].

Independent from the mechanisms responsible for the irradiation-induced dimensional change is the mechanisms governing irradiation creep, which is defined as the difference in the amount of dimensional change between a loaded sample and an unloaded sample. The mechanism of irradiation creep in nuclear graphite significantly relieves internal stresses during operation. Without the irradiation creep response, graphite components would fail within a few years of operation [21]. Macroscopically, compressive strains will result in a net increase in the amount of dimensional change, in contrast tensile strains will result in a decrease in the amount of dimensional change when compared to an unstressed control sample [22]. On the atomic scale, the fundamental mechanism of irradiation creep remains somewhat contentious. Historically irradiation creep has been attributed to dislocation glide and basal slip activated by neutron bombardment along with the annihilation and creation of pinning points interstitially [23]. On the other hand, a more recent analysis of creep data produced by Kennedy in 1966 [24] contradicted the pinning / unpinning model. Analysis showed that the steady-state creep rate was linear in dependence to the applied stress, thus suggesting a climb mechanism for dislocations [25]. A consensus on either model remains elusive as both models lack definitive microstructural evidence.

To test these and future theories, detailed experimental data describing the change in physical properties of the graphite is a necessity. Understanding the physics behind different material properties and the changes that occur to those properties during irradiation allows the theories and models to be tested. Models that can describe and support the physical changes that are a result of neutron-irradiation, must also work for the reverse process of annealing those changes by raising the material temperature above the irradiation temperature. This paper seeks to provide both the change in properties due to neutron-irradiation and the recovery of those properties during thermal annealing. The properties investigated here for both irradiation damage and isothermal - isochronal annealing are: dimensional change, electrical resistivity, Young's modulus of elasticity, coefficient of thermal expansion and thermal diffusivity. The graphite specimens used for this study are from the US Department of Energies (DOE) Advanced Reactor Technologies (ART) Materials Research and Development program's second irradiation capsule, AGC-2.

2. Experimental Program

The ART Program is conducting an extensive graphite irradiation experiment to provide data for licensing of a high temperature reactor (HTR) design. New nuclear graphite grades have been developed and are considered suitable candidates for new HTR reactor designs. To support the design and licensing of HTR core components within a commercial reactor, a complete properties database must be developed for these current grades of graphite. Quantitative data on in-service material performance is required for the physical, mechanical, and thermal properties of each graphite grade, with a specific emphasis on data accounting for the life-limiting effects of irradiation creep on key physical properties of the HTR candidate graphite grades.

Within the ART program the Advanced Graphite Creep (AGC) experiment is currently being conducted to determine the in-service behavior of these new graphite grades for HTR. Irradiation data are provided through the AGC test series that is comprised of six planned capsules irradiated in the Advanced Test Reactor (ATR) at Idaho National Laboratory (INL). The AGC irradiation conditions are similar to the anticipated environment within a high-temperature core design. Each irradiation capsule is composed of more than 400 graphite specimens that are characterized before and after irradiation to determine the irradiation-induced changes in material properties and the rate of life-limiting irradiation creep for each graphite grade.

In addition to determining the irradiation-induced changes to the material properties of selected nuclear graphite grades, the AGC experiment dedicates a significant amount of scope to determining rates of irradiation-induced creep for different nuclear graphite grades. The traditional method for measuring irradiation-induced creep is to apply a significant mechanical load (inducing a mechanical stress within the graphite) to half the specimens during irradiation while leaving the remaining half of the specimens unloaded (unstressed). Mechanically loaded (stressed) specimens are traditionally designated as the creep specimens, and the unloaded (unstressed) specimens are designated as the control specimens. The resulting difference in dimensional change between the loaded and unloaded specimens (assuming that temperature and dose levels are the same) provides the amount of irradiation-induced strain for each “matched pair” of graphite specimens.

To provide all necessary material property tests in the AGC experiments, each test series capsule contains “creep” specimens that are stressed at three different levels during the irradiation, 13.8, 17.2 and 20.7 MPa. Control specimens are not stressed, and the dimensional change of the creep and control specimens is used to determine the creep coefficient as a function of stress, dose

and irradiation temperature. “Piggyback” specimens provide thermal material property behavior for the different grades of graphite. These piggyback specimens are not mechanically loaded and are subjected only to neutron irradiation.

All specimens are 12.7 mm (0.5 in.) in diameter, with the larger creep and control specimens being 25.4 mm (1.0 in.) long and the button-sized piggyback specimens being 6 mm (0.25 in.) long. The large creep and control specimens provide accurate dimensional change, elastic modulus, thermal expansion, electrical resistivity, and mechanical strength measurements. However, the longer creep specimens make them unsuitable for thermal diffusivity measurements. The small piggyback specimens permitted only dimensional measurements, density testing, and thermal-diffusivity testing to be performed. Together, both types of specimens provide the changes in material properties for stressed and unstressed graphite grades.

Unless otherwise specified, the specimen dose and irradiation temperature range for the data contained here is 2.5 to 4.7 dpa and 540 to 680°C respectively. These ranges are a result of the flux profile and cooling design of the experiment capsule. This is not to say that the temperature and flux varied during the irradiation experiment but rather that the individual specimens were irradiated at various constant temperatures and fluxes within this range. The three graphite grades chosen for the annealing experiments cover a wide range of manufacturing and forming process, coke source, and grain size, Table 1. Additionally, Table 2 shows the number of samples used in this work for each stress condition.

Table 1: *Graphite types used.*

Grade	Coke source	Grain size	Forming Process	Vendor
PCEA	Petroleum	Med.	Extrusion	Graftech, USA
NBG-18	Pitch	Med.	Vibration Molding	SGL, Germany
IG-110	Petroleum	Fine	Isostatic Pressed	ToyoTanso, Japan

Table 2: *Sample size for each stress condition.*

	0 MPa	13.8 MPa	17.2 MPa	20.7 MPa
PCEA	24	8	8	8
NBG-18	18	6	6	6
IG-110	17	6	6	6

3. Material Property Data

All measurements were made according to the applicable American Society of Testing and Materials (ASTM) standards. The specific standard for each measurement is called out in the corresponding section below. Further details of how these measurement standards are applied to the graphite specimens can be found in INL/EXT-17-41165 [26][NO_PRINTED_FORM]. This report describes the measurement techniques, equipment, and standards used to gather data analyzed here. Additionally, Ref.[26] thoroughly describes the design and the as-run irradiation conditions of AGC-2.

Annealing was conducted in a Thermal Technology Furnace (model 1000 3560 FP20) with a ramp rate of 5°C/min from room temperature to 400°C. The temperature was held at 400°C for 12 min while backfilling the chamber with UHP He and allowing the vacuum pressure to stabilize (ca. 190 mT). The ramp rate was then increased to 20°C/min until annealing temperature followed by a cooling rate of 20°C/min to 150°C. Annealing experiments were carried out consistently for all data reported here. A minimum of one specimen of each particular geometry, graphite type, and stressed condition was annealed at the specified constant temperatures between 500°C and 2380°C for 24 hours in a stepwise manner. Unfortunately, during the last annealing cycle of NBG-18, INL's radiological control staff reported a contamination issue in the lab and the annealing cycle was terminated. Following each annealing step, the specimen's material properties were measured and compared to the unirradiated value, typically by normalizing the annealed value with the unirradiated value.

3.1. *Irradiation Induced Dimensional Changes and Creep*

The phenomenon of irradiation-induced creep within graphite has been shown to be critical in determining the total useful lifetime of graphite components. Irradiation-induced creep occurs under the simultaneous application of neutron irradiation and applied stresses within the graphite components. This creep or relaxation of the graphite can help to accommodate the significant internal stresses within graphite components that arise from irradiation induced dimensional changes, differential thermal expansion, and externally applied loads. Irradiation-induced creep relaxes these large internal stresses, thus reducing the risk of crack formation and component failure. Higher levels of irradiation creep will relieve more internal stress providing the components longer useful lifetimes within a reactor core.

The mechanism to describe irradiation creep is independent from graphite dimensional change due to irradiation only. To date, there remains to be a consensus on a creep mechanism. Historically, irradiation creep has been attributed to the pinning and un-pinning of dislocations (i.e., glide or slide) [23]; however, more recent research contradicts the aforementioned model in which analysis of historical data suggests the mechanism is due to dislocation climb [25,27]. Fig.1 shows the percent dimensional change for graphite grades NBG-18, IG-110, and PCEA as a function of the applied stress for specimens irradiated between 600°C and 675°C and a dose range of 3.7 to 4.5 dpa. The dimensional change was measured according to ASTM C559 [28] with a Mitutoyo digital micrometer (model 121-115). The change in specimen length for those that were not stressed falls in a narrow band between 0.75 and 1.0 percent. This small change drastically increases when the specimens are compressively stressed. The level of radiation-induced creep is different for the three grades of graphite with PCEA graphite exhibiting a maximum deformation of over 3%. This data is consistent with historical compressively loaded creep data [22,23,25,29].

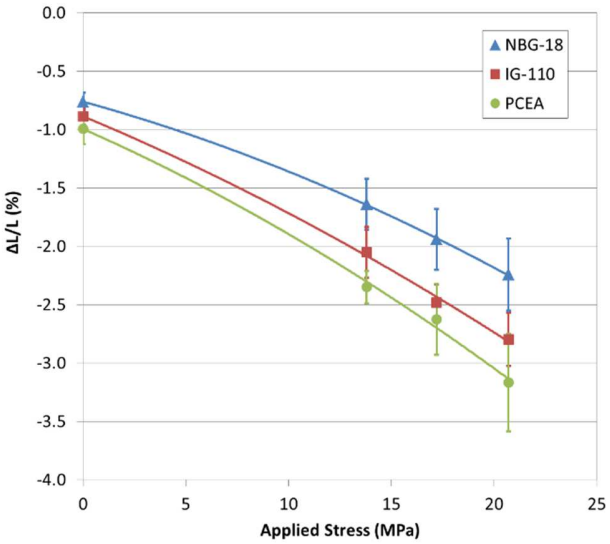

Fig.1. *Irradiation dimensional change and creep as a function of applied stress for 3 different grades of graphite. (A color version of this figure can be viewed online.)*

Two specimens of each graphite type were annealed at the temperatures shown in Fig.2. Both unstressed and stressed specimens were evaluated. The unstressed specimens showed no dimensional recovery up to a temperature of 2380°C and the stressed specimens of IG-110 and PCEA only showed a small amount of recovery starting at an annealing temperature of 1500°C.

Again, this behavior is consistent with theorized closure of cracks and porosity in the graphite microstructure due to *c*-axis expansion, resulting in densification [29,30] As the neutron damaged graphite is annealed at higher temperatures, only the atomic level defects are repaired, thus significant dimensional recovery is not be expected.

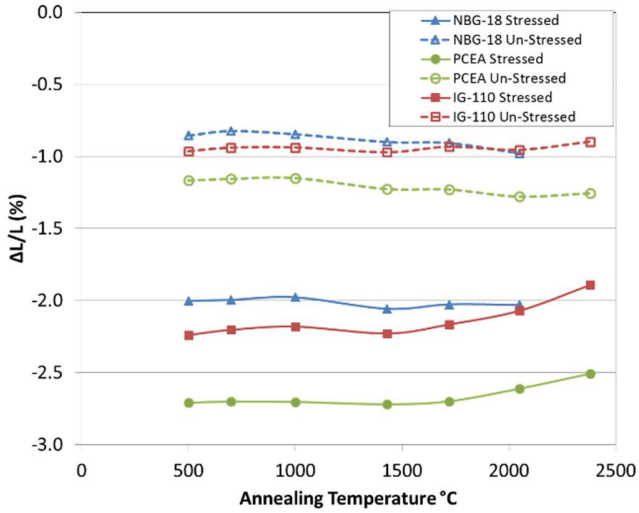

Fig.2. *The effect of thermal annealing on the irradiation induced dimensional changes for the three different graphite grades. Solid symbols indicate specimens that were stressed at 20.7 MPa during the irradiation. Hollow symbols represent unstressed specimens. (A color version of this figure can be viewed online.)*

3.2. Young's Modulus

A material's elastic moduli are a measure of how compliant (or stiff) the material behaves and is useful for ascertaining a graphite grade's mechanical properties, irradiation creep response, and the structural strength and integrity of graphite components. Measured fundamental resonant frequency, specimen dimensions, and mass are used to calculate Young's modulus in accordance with ASTM C747 [31]. This test method measures the fundamental resonant frequency of test specimens of suitable geometry by exciting them mechanically with a singular elastic strike. Specimen supports, impulse locations, and signal pick-up points are selected to induce and measure specific modes of the specimen vibration. The transient signals are analyzed, and the fundamental resonant frequency is isolated by a signal analyzer.

In Fig.3 the average change in Young's modulus due to irradiation is shown for the three different graphite types as a function of stress applied to the specimens. Variation in the data is a result of the different variables within the experiment, including irradiation temperature, dose and

grain orientation and is represented by the ±1 standard deviation error bars. The overall increase in modulus is significant with that of IG-110 being almost double the unirradiated condition. Modulus change for all graphite grades gradually decreases as the applied stress (and the resulting sustained creep strain) is increased. Stressed specimens exhibiting larger plastic strain are shown to experience less change in modulus than the unstressed control specimens that show less plastic strain.

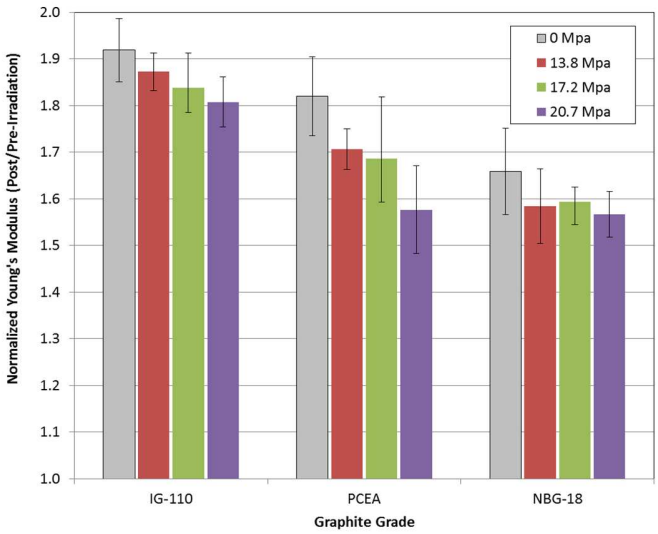

Fig.3. *A comparison between different graphite grades of the increase in Young's modulus as a function of applied stress during irradiation. (A color version of this figure can be viewed online.)*

During annealing, reduction in the irradiation-induced high modulus begins to occur at temperatures above ~700°C, Fig.4, and is nearly fully recovered to the original unirradiated modulus by 2380°C. Due to the lack of dimensional recovery with annealing, it is thought that few if any cracks or pores are recovered. This is consistent with the incomplete recovery of the modulus. Based on the full recovery of the thermal diffusivity (shown below) it is surmised that the atomic level defects are completely annealed out at a temperature of 2380°C, therefore consistent with the near full recovery of the elastic modulus. Only the contribution of the changes in cracks and porosity is missing from fully re-establishing the compliance of the graphite to the unirradiated condition.

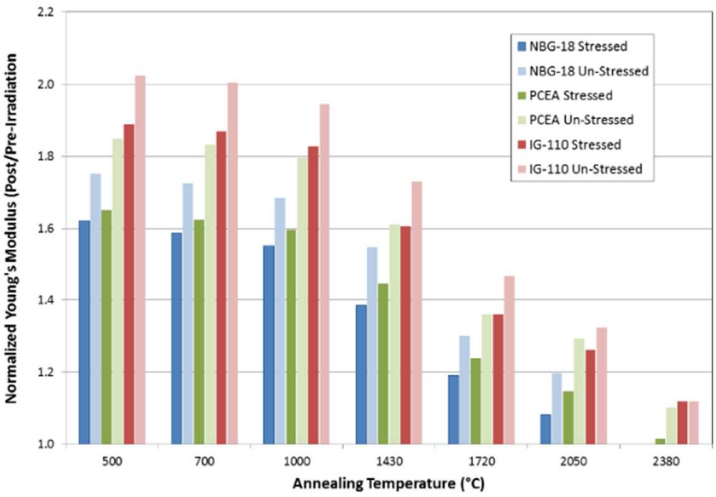

Fig.4. *Recovery of elastic modulus in irradiated graphite as a function of the annealing temperature. (A color version of this figure can be viewed online.)*

3.3. Electrical Resistivity

Electrical resistivity is used as a rapid, simple means for determining the isotropy or grain orientation of manufactured graphite. Changes in electrical resistivity due to irradiation can be used to ascertain the level of defects as well as the type of defects that develop at various irradiation temperatures [32]. Resistivity is measured following ASTM C 611 [33]. The measurement technique is commonly referred to as four-point probe. It consists of passing a known current through the sample and measuring voltage across the sample at known locations.

While there are significant similarities between all tested specimens, there are some differences between the different graphite grades. Fig. 5 illustrates the effects on electrical resistivity from irradiation as a function of stress in the specimen during irradiation. The change in resistivity is normalized by the unirradiated value and the error bars represent ±1 standard deviation in the group of approximately 20 specimens. On average, resistivity changes for all graphite grades remained relatively constant across the increasing applied stress. It appears resistivity changes for unstressed specimens may be slightly higher than stressed specimens for all graphite grades, but the difference is small and within the one standard deviation error bars. Still, the change in electrical resistivity for the three grades of graphite tested is significant. The extruded PCEA specimens demonstrated nearly a 200% increase in resistivity, while the IG-110 specimens exhibit the least change of approximately 125%. As mentioned above, when graphite is exposed

to fast neutron radiation, carbon atoms are knocked out of there equilibrium positions in the lattice structure to form a vacancy and interstitial pair (Frenkel pair). At higher irradiation temperatures these simple defects grow into more complex formations of interstitial atoms and basal plane vacancies [13,15]. Also, as the dose of neutrons builds so does the complexity and number of defects formed [13]. These defects decrease mobility of the electrons by acting as scattering sites and, the more complex defects, can even trap electrons. Together a significant increase in electrical resistivity is seen.

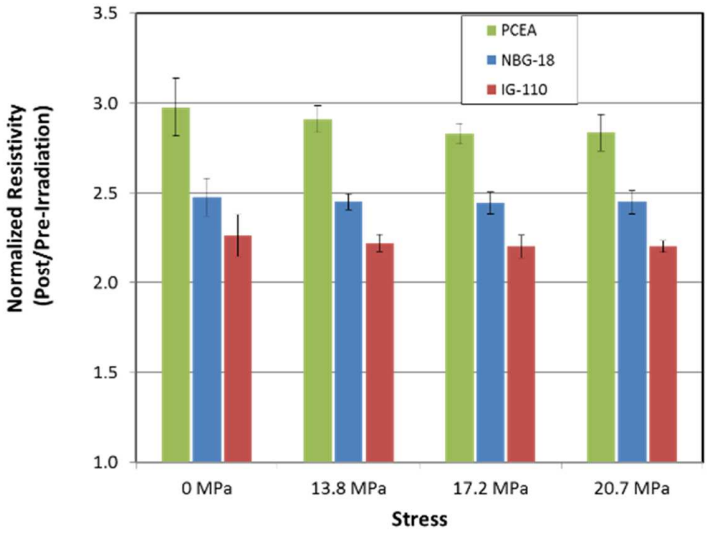

Fig.5. *The change in electrical resistivity due to irradiation relative to the unirradiated condition. 3 graphite types are shown as a function of stress during irradiation. (A color version of this figure can be viewed online.)*

Thermal annealing of the irradiated graphite at high enough temperatures should increase the electrical conductivity by rearranging carbon atoms back to their lower energy states and when the annealing temperature is near the graphitization temperature the basal plane hexagonal formation will be reformed that is efficient in electron transfer. Fig. 6 shows the effect of annealing on the change in irradiation up to a temperature of 2380°C for both the stressed and unstressed specimens. Starting at 1430°C there is an obvious decline for all graphite grades and conditions. Both stressed and unstressed specimens decline at nearly the same rate. Although typically seen when annealing graphite that has been irradiated at lower temperatures than was done here, there is a slight increase in resistivity up to ~1000°C. This has been attributed to the changes in defect

structure when vacancies become increasingly mobile and coalesce to produce effective electron traps that reduce the charge carrier density [32,34,35].

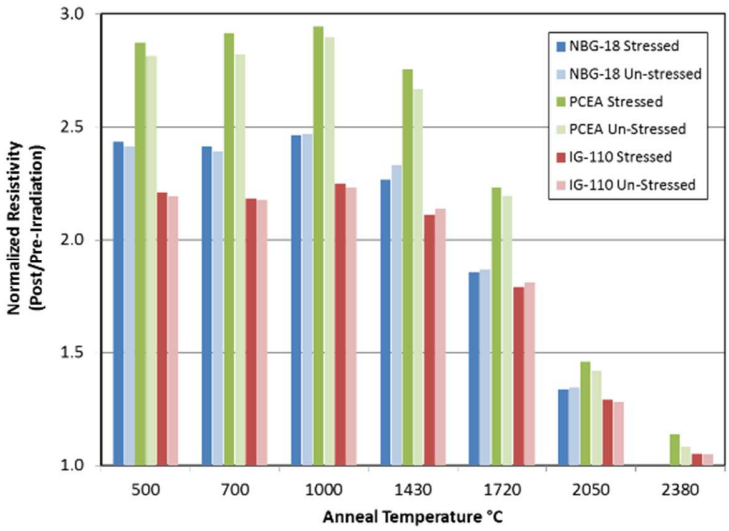

Fig.6. *The effect of annealing temperature on electrical resistivity for three graphite grades, stressed at 20.7MPa and un-stressed. (A color version of this figure can be viewed online.)*

3.4. Coefficient of Thermal Expansion

The coefficient of thermal expansion (CTE) defines how the physical size of an object changes with a change in temperature. Specifically, it measures the fractional change in size per degree change in temperature at a constant pressure. CTE is a key parameter for determining thermally induced stress states, volumetric changes, and irradiation creep rates within graphite reactor core components.

CTE is measured here in accordance with ASTM E228-06. This test method uses a push-rod dilatometer to determine the change in length of a graphite specimen relative to that of the holder as a function of increasing/decreasing temperature. The temperature is varied over the desired range at a slow constant heating or cooling rate. Using calibration to subtract the growth of instrument fixtures, the change in specimen length is recorded as a function of temperature. The mean CTE is calculated from the slope of a line drawn from the reference temperature, typically 20°C, and a specified temperature. This is performed for specific temperatures covered by the growth curve to produce mean CTE values. CTE was measured at successive 100°C increments over the temperature range of 100 to 500°C. The upper temperature limit of 500°C is set by the nominal irradiation temperature of 600°C to prevent the influence of annealing in the CTE data.

Fig. 7 illustrates the irradiation induced CTE changes of the three graphite grades. The small-grained, iso-molded grade of IG-110 demonstrates the largest CTE increase while the larger grained NBG-18 and PCEA have less of an increase. It is important to note that each data point at the discreet material temperature is the average of approximately 20 specimens that cover the full temperature and dose range of the AGC-2 experiment capsule. Stress in the specimens makes a significant difference in increasing the average CTE at all material temperatures up to 500°C. Also note that each of the stressed data points is an average of all 3 stress levels applied in the AGC experiment. Error bars represent ±1 standard deviation from the mean.

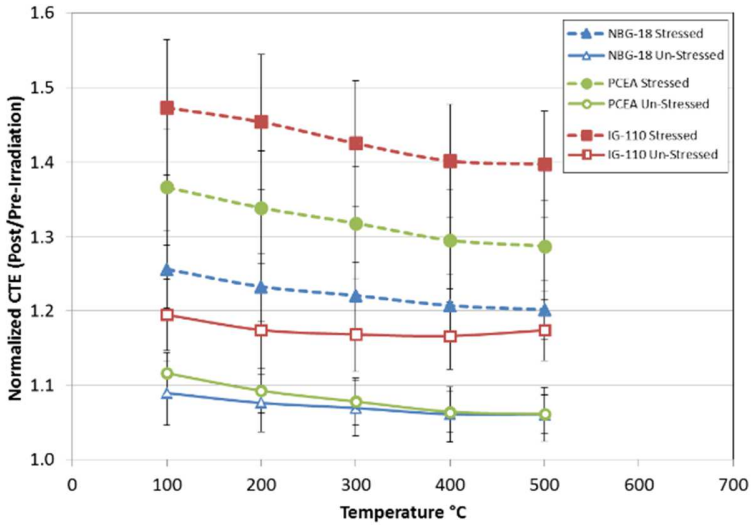

Fig.7. *Normalized coefficient of thermal expansion for NBG-18, IG-110 and PCEA as a function of material temperature for both the irradiated and unirradiated conditions. (A color version of this figure can be viewed online.)*

The effect of stress on the percent change in CTE was investigated further in Fig.8. This data represents the increase in CTE as a function of the 3 distinct stress levels at a material temperature of 500°C. Error bars represent ±1 standard deviation from the mean. The large CTE difference between stressed and unstressed specimens is immediately observed. As an example, an un-stressed specimen of PCEA had a ~6% increase, while the specimen stressed at 20.7 MPa had an increase of ~32%. The increase in CTE in graphite irradiated was described by Sutton and Howard in 1962 [36] and commonly seen in later publications [37–39]. In a polycrystalline graphite as much as 37% of the thermal expansion can be attributed to the expansion of the crystallites along the *c*-axis. In addition, when graphite is irradiated, some of the porosity and cracks that accommodate the crystallite expansion are closed up. With the addition of stress during

irradiation the creep strain experienced in the graphite continues to densify the graphite and decrease the accommodation cracks and porosity which in turn results in the bulk thermal expansion being significantly higher.

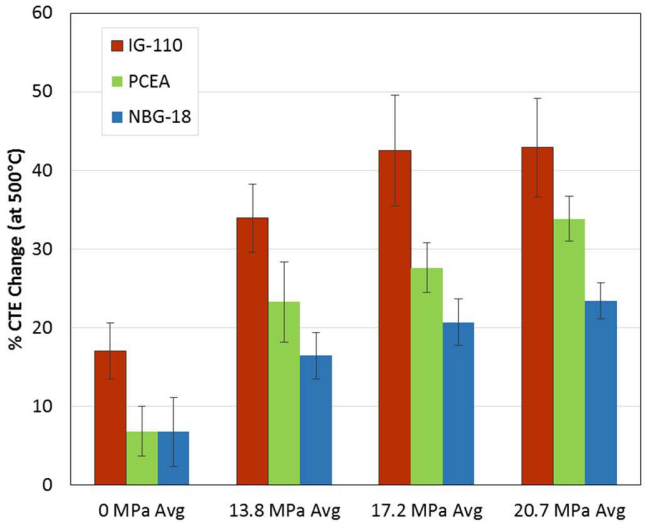

Fig.8. *Percent change in CTE for the three graphite grades, comparing the effects of stress in the graphite during irradiation at a material temperature of 500°C. (A color version of this figure can be viewed online.)*

What is unclear is the response of bulk CTE to thermal annealing. Fig.9 shows significant, but not full, recovery up to an annealing temperature of 2380°C. If the increase in CTE due to irradiation is predominately a function of densification during irradiation, the annealing process would need to form cracks and pores that would accommodate the expansion as in the unirradiated material. If cracks and pores are forming, one would surmise that the graphite would also recover dimensionally. This is contradictory to Fig.2 (that shows little to no dimensional recovery) unless the cracks and pores are of a size and distribution that would accommodate thermal growth of the crystallites but not result in recovery of bulk dimensions. As the graphite is cycled thermally during the annealing experiment it is possible that differential thermal expansion due to varying crystallite orientation would cause micro cracking and at temperatures near the graphitization temperature.

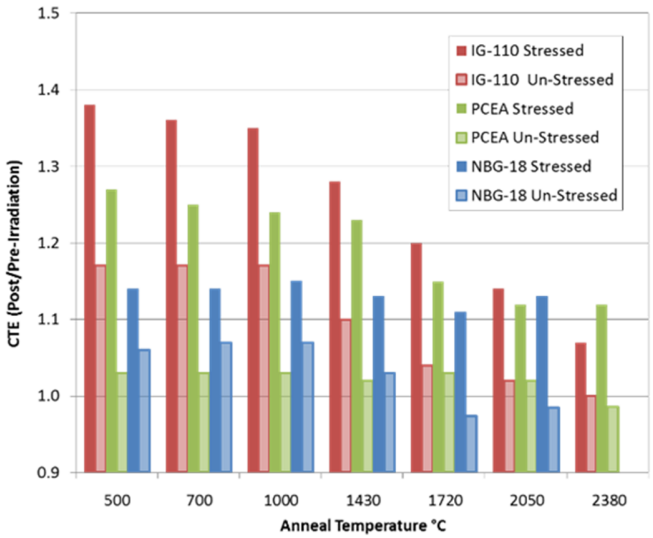

Fig. 9. *Normalized CTE for the three graphite grades as a function of annealing temperature and stress during irradiation. (A color version of this figure can be viewed online.)*

3.5. Thermal Diffusivity

Thermal conductivity and diffusivity are the most important thermophysical material parameters for describing the heat transport properties of a graphite component. Thermal diffusivity is a measure of the rate of heat transfer in a material (i.e., how fast heat is transferred from the hot side to the cold side of a material). It is useful for ascertaining heat conduction through the graphite core for passive decay heat removal, calculations of thermal stresses, and modeling core physics in a graphite moderated design.

The thermal diffusivity measurements were carried out in accordance with ASTM C714-17. This measurement is performed on small, thin, disk-shaped specimens. A pulsed laser is used to subject one surface of the specimen to a high-intensity, short-duration energy pulse. The energy of this pulse is absorbed on the front surface of the specimen and the resulting rise in rear-face temperature is recorded. Thermal diffusivity is calculated from the specimen thickness and the time required for the rear face temperature to reach 50% of its maximum value.

Thermal diffusivity is a strong function of the graphite temperature and is therefore measured as a function of material temperature, Fig.10. Because of the physical limitations necessary to conduct diffusivity measurements, i.e., a relatively thin specimen, the measurements were made on the piggyback specimens only and none of the piggyback specimens were subjected to an applied mechanical stress during irradiation. Therefore, there are no data comparing the

effects of different stress levels (and induced accelerated strains). With the exception of the PCEA sample in Fig.10, diffusivity was measured at successive 100°C increments over the temperature range of 100 to 500°C. To prevent the influence of annealing on the diffusivity data, the upper-temperature limit of 500°C was determined by the nominal irradiation temperature of 600°C.

Diffusivity in graphite is normally expected to gradually reduce as the material testing temperatures increase due to grain boundary and Umklapp scattering effects [2,40] Grain boundary phonon scattering dominates thermal resistance at low temperatures but becomes insignificant above a few hundred degrees Celsius while the Umklapp scattering dominates at higher temperatures and defines the upper limit to the thermal conductivity for a "perfect crystalline" graphite. This gradual reduction due to phonon scattering effects is observed in both pre and post-irradiated data.

The reduction in diffusivity due to irradiation is commonly described as a result of phonon scattering from defects that form in the graphite lattice. Depending on the irradiation temperature these defects can range from single interstitial atoms and vacancies in the basal planes at low irradiation temperatures ($T_{irr} \leq 200$°C) to more complex clusters of interstitials and vacancies that form due to their mobility at higher temperatures. In either case, the phonon scattering is thought to be dominated by defects in the basal planes *a*-axis [41].

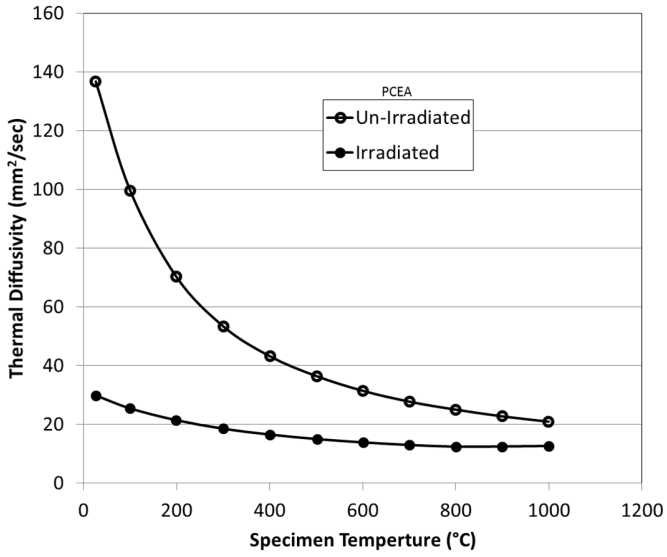

Fig.10. *The behavior of thermal diffusivity in PCEA as a function of the material temperature for irradiated and unirradiated graphite.*

Fig. 11 shows the ratio of average pre- and post-irradiation diffusivity for graphite grades IG-110, PCEA and NBG-18 as a function of measurement temperature. As with the other material property measurements, the change in thermal diffusivity was substantial. At a material temperature of 100°C the post irradiated diffusivity is approximately 25% of the unirradiated value and at a material temperature of 500°C the post irradiation diffusivity is 40%. The error bars represent one standard deviation in the data, reflecting the different variables within the experiment, including irradiation temperature and dose.

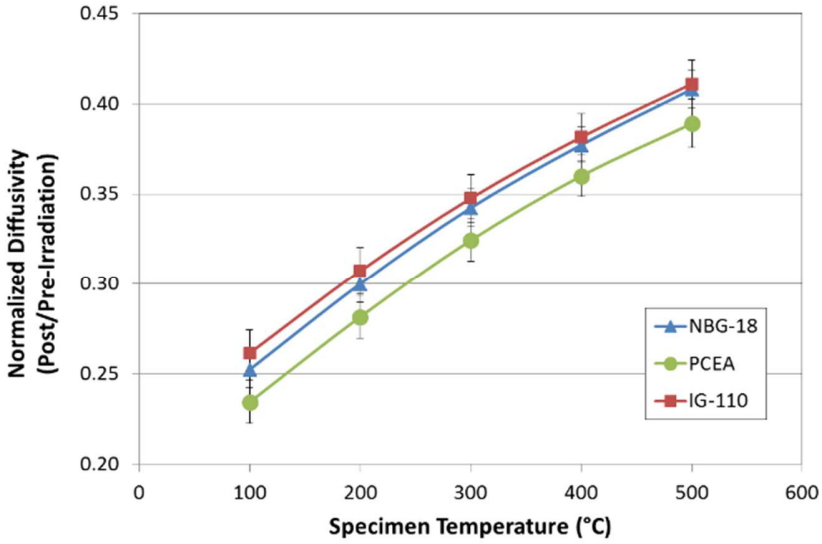

Fig.11. *The effect of radiation damage on three different graphite grades as a function of the material test temperature. (A color version of this figure can be viewed online.)*

In Fig.12, a small group of specimens from each of the three grades of graphite was selected with a narrow range of irradiation temperatures (600 ± 50°C) in order to examine the effect of irradiation dose. Their reduction in diffusivity is plotted as a function of irradiation dose at material test temperatures of 100°C and 500°C. Over the dose range of 2.0 to 4.5 all three grades trend to lower diffusivities as the dose is increased indicating the continued formation of phonon scattering defects. The trend of lower diffusivities as irradiation dose is increased agrees with previous studies by others these results agree with studies by others conducted [38,39]. The rate of decrease is similar for both the low material temperature of 100°C that is dominated by grain boundary scattering and the higher Umklapp dominated material temperature of 500°C. This similar reduction in conductivity at the two temperatures would indicate that a similar mechanism is responsible for this reduction, the obvious being increased defect density in the basal planes [41].

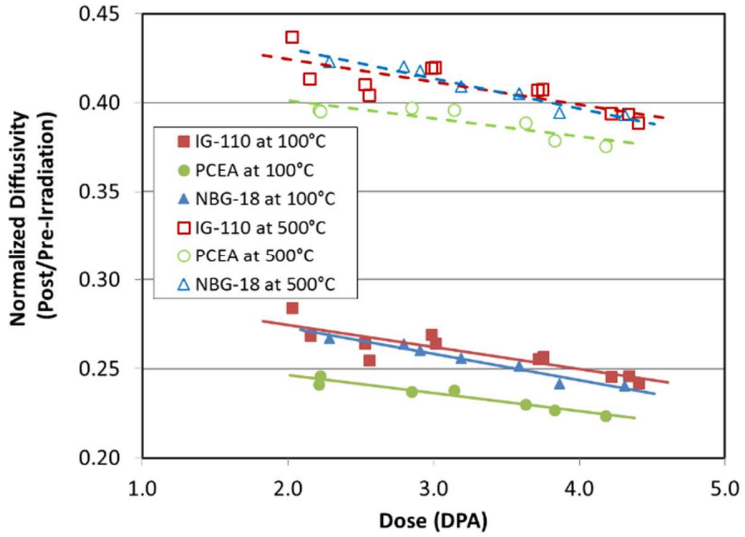

Fig.12. *Reduction in thermal diffusivity at material test temperatures of 100°C and 500°C as a function of irradiation dose at an irradiation temperature of 600 ± 50°C. (A color version of this figure can be viewed online.)*

The effects of annealing on the reduction of thermal diffusivity due to irradiation are seen in Fig.13. Two irradiation dose levels are represented. As seen previously, specimens at the higher dose have increased resistance to heat transfer. This trend continues consistently throughout the range of annealing temperatures. It is not until an annealing temperature of 1000°C that the energy threshold is met for the reduction of phonon scattering defects in the graphite. The rate of defect repair as a function of annealing temperature remains constant up to 2380°C at which point only the lower dose specimens have fully recovered their original values of thermal diffusivity.

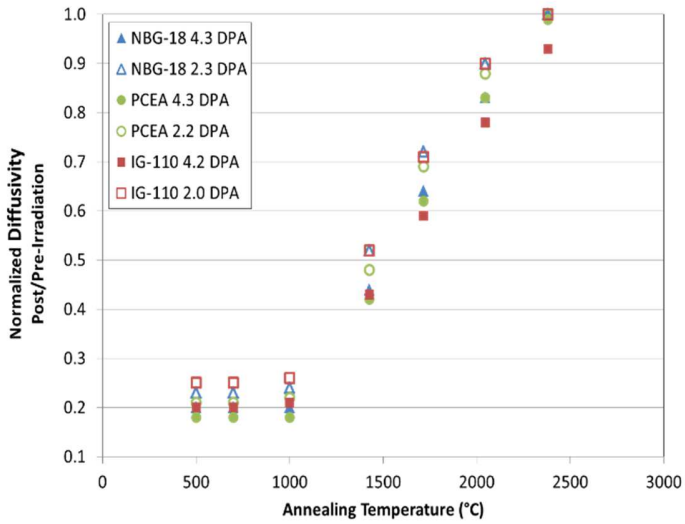

Fig.13. *Thermal diffusivity recovery as a function of annealing temperature. (A color version of this figure can be viewed online.)*

4. Summary and Observations

This paper seeks to provide both the change in properties in nuclear grade graphite due to neutron irradiation and the recovery of those properties during thermal annealing. The properties investigated here for both irradiation damage and isothermal - isochronal annealing are: dimensional change, electrical resistivity, Young's modulus of elasticity, coefficient of thermal expansion and thermal diffusivity. These properties are investigated as a function of irradiation dose, temperature, stress and annealing temperature.

The change in specimen length for unstressed specimens falls in a narrow band between 0.75 and 1.0 percent. This small change drastically increases when the specimens are compressively stressed. The level of radiation induced creep is different for the three grades of graphite with PCEA graphite exhibiting a maximum deformation in length of over 3%. The annealed unstressed specimens showed no dimensional recovery up to a temperature of 2380°C and the stressed specimens of IG-110 and PCEA showed only a very small amount of recovery starting at an annealing temperature of 1500°C. This lack of dimensional recovery has been attributed to only atomic level defects being repaired during the annealing process. It is possible that some level of Mrozowski and differential thermal expansion cracks formed at the upper annealing temperatures during the heating cycles that resulted in the slight dimensional recovery of IG-110 and PCEA. Although no micrographs were prepared for this study, recent microscopy studies on high-temperature annealing of IG-110 found the formation of fullerene-like defects to

be a direct result of annealing at 2500°C [42]. The formation of such defects was proposed to be a mechanism for non-recoverable physical properties in irradiated graphites [42].

The overall increase in Young's modulus is significant with that of IG-110 being almost double the unirradiated condition. Modulus change for all graphite grades gradually decreases as the applied stress (and the resulting sustained creep strain) is increased. Stressed specimens exhibiting larger plastic strain are shown to experience less change in modulus than the unstressed control specimens exhibiting smaller plastic strain. During annealing, reduction in the irradiation induced higher modulus begins to occur at temperatures above ~700°C and nearly recovers to the original unirradiated modulus by 2380°C. Due to the lack of dimensional recovery with annealing it is thought that few if any cracks or pores are recreated. This is consistent with the incomplete recovery of the modulus.

The change in electrical resistivity for the three grades of graphite tested is significant. The extruded PCEA specimens demonstrated nearly a 300% increase in resistivity, while the IG-110 specimens changed the least at 225%. Resistivity changes for all graphite grades remained relatively constant with increasing applied stress. Reduction in resistivity during thermal annealing started at 1000°C for all graphite grades with both stressed and unstressed specimens declining at nearly the same rate.

All grades of graphite studied showed an increase between 5% and 20% in CTE due to irradiation with dose levels below that expected for turnaround. Stress during irradiation greatly increased the change in CTE to a range between +20% for NBG-18 to 48% for IG-110. The increase for unstressed specimens is explained by the reduction in accommodation cracks and pores. This effect is only magnified by irradiation strain when the specimens are under a compressive stress. Thermal annealing begins to recover the unirradiated CTE at temperatures above 500°C but it remained incomplete for stressed specimens even at 2380°C. There is little to no recovery of dimensional change during annealing, indicating that the annealing process is primarily at an atomic level and significant cracks and pores are not created. This is in contrast to the near complete recovery of the CTE during annealing.

As with the other material properties of graphite, the change in thermal diffusivity was substantial. At a material temperature of 100°C the post irradiated diffusivity is approximately 25% of the unirradiated value and at a material temperature of 500°C the post irradiation diffusivity is 40%. Over the dose range of 2.0 to 4.5 at an irradiation temperature of 600 ± 50°C, all three

grades trend to lower diffusivities as the dose is increased indicating the continued formation of phonon scattering defects. The rate of decrease is similar for both the low material temperature of 100°C, which is dominated by grain boundary scattering, and the higher Umklapp scattering dominated material temperature of 500°C. This similar reduction in conductivity, as a function of irradiation dose, would indicate that a mechanism unrelated to Umklapp or grain boundary scattering is at play and is most likely an increase in irradiation induced defect densities in the basal planes. It is not until an annealing temperature of 1000°C that the energy threshold is met for the reduction of phonon scattering defects in graphite. The rate of defect repair as a function of annealing temperature remains constant up to 2380°C at which point only the lower dose specimens have fully recovered their original values of thermal diffusivity.

Acknowledgements

The authors would like to acknowledge retiree, David W. Swank for his contributions to this work. The authors would like to acknowledge that funding for this work was provided by the U.S. Department of Energy's Advanced Reactor Technologies Program under the DOE Idaho Operations Office, Contract DE-AC07-05ID14517, with Battelle Energy Alliance, LLC.

References

[1] R.H. Telling, M.I. Heggie, Radiation defects in graphite, Philosophical Magazine. 87 (2007) 4797–4846. https://doi.org/10.1080/14786430701210023.

[2] B.T. Kelly, Physics of Graphite, Applied Science Publishers, London, 1981.

[3] T. Tanabe, Radiation damage of graphite - degradation of material parameters and defect structures, Phys Scr. T64 (1996) 7–16. https://doi.org/10.1088/0031-8949/1996/T64/001.

[4] J. Koike, D.F. Pedraza, Dimensional changes in highly oriented pyrolytic graphite due to electron-irradiation, J Mater Res. 9 (1994) 1899–1907. https://doi.org/10.1557/JMR.1994.1899.

[5] S. Muto, T. Tanabe, Damage process in electron-irradiated graphite studied by transmission electron microscopy. I. High-resolution observation of highly graphitized carbon fibre, Philosophical Magazine A. 76 (1997) 679–690. https://doi.org/10.1080/01418619708214029.

[6] C. Karthik, J. Kane, D.P. Butt, W.E. Windes, R. Ubic, In situ transmission electron microscopy of electron-beam induced damage process in nuclear grade graphite, Journal of Nuclear Materials. 412 (2011) 321–326. https://doi.org/10.1016/j.jnucmat.2011.03.024.

[7] H.M. Freeman, A.J. Scott, R.M.D. Brydson, Thermal annealing of nuclear graphite during in-situ electron irradiation, Carbon N Y. 115 (2017) 659–664. https://doi.org/10.1016/j.carbon.2017.01.057.

[8] S. Muto, S. Horiuchi, T. Tanabe, Local structural order in electron-irradiated graphite studied by high-resolution high-voltage electron microscopy, J Electron Microsc (Tokyo). 48 (1999) 767–776. https://doi.org/10.1093/oxfordjournals.jmicro.a023747.

[9] J.A. Hinks, A.N. Jones, A. Theodosiou, J.A. van den Berg, S.E. Donnelly, Transmission Electron Microscopy Study of Graphite under *in situ* Ion Irradiation, J Phys Conf Ser. 371 (2012) 012046. https://doi.org/10.1088/1742-6596/371/1/012046.

[10] C.I. Contescu, J.D. Arregui-Mena, A.A. Campbell, P.D. Edmondson, N.C. Gallego, K. Takizawa, Y. Katoh, Development of mesopores in superfine grain graphite neutron-irradiated at high fluence, Carbon N Y. 141 (2019) 663–675. https://doi.org/10.1016/j.carbon.2018.08.039.

[11] S. Johns, T. Poulsen, J.J. Kane, W.E. Windes, R. Ubic, C. Karthik, Formation of carbon nanostructures in nuclear graphite under high-temperature in situ electron-irradiation, Carbon N Y. 143 (2019) 908–914. https://doi.org/10.1016/j.carbon.2018.11.077.
[12] D. Liu, D. Cherns, S. Johns, Y. Zhou, J. Liu, W.Y. Chen, I. Griffiths, C. Karthik, M. Li, M. Kuball, J. Kane, W. Windes, A macro-scale ruck and tuck mechanism for deformation in ion-irradiated polycrystalline graphite, Carbon N Y. 173 (2021) 215–231. https://doi.org/10.1016/j.carbon.2020.10.086.
[13] S. Johns, L. He, K. Bustillo, W.E. Windes, R. Ubic, C. Karthik, Fullerene-like defects in high-temperature neutron-irradiated nuclear graphite, Carbon N Y. 166 (2020) 113–122. https://doi.org/10.1016/j.carbon.2020.05.028.
[14] C. Karthik, J. Kane, D.P. Butt, W.E. Windes, R. Ubic, Neutron irradiation induced microstructural changes in NBG-18 and IG-110 nuclear graphites, Carbon N Y. 86 (2015) 124–131. https://doi.org/10.1016/j.carbon.2015.01.036.
[15] R.H. Telling, C.P. Ewels, A.A. El-Barbary, M.I. Heggie, Wigner defects bridge the graphite gap, Nat Mater. 2 (2003) 333–337. https://doi.org/10.1038/nmat876.
[16] J.G. McHugh, P. Mouratidis, A. Impellizzeri, K. Jolley, D. Erbahar, C.P. Ewels, Prismatic edge dislocations in graphite, Carbon N Y. 188 (2022) 401–419. https://doi.org/10.1016/j.carbon.2021.11.072.
[17] J.G. McHugh, P. Mouratidis, K. Jolley, Ripplocations in layered materials: Sublinear scaling and basal climb, Phys Rev B. 103 (2021). https://doi.org/10.1103/PhysRevB.103.195436.
[18] M.W. Barsoum, Ripplocations: A Progress Report, Front Mater. 7 (2020). https://doi.org/10.3389/fmats.2020.00146.
[19] M.I. Heggie, I. Suarez-Martinez, C. Davidson, G. Haffenden, Buckle, ruck and tuck: A proposed new model for the response of graphite to neutron irradiation, Journal of Nuclear Materials. 413 (2011) 150–155. https://doi.org/10.1016/j.jnucmat.2011.04.015.
[20] S. Johns, L. He, J.J. Kane, W.E. Windes, R. Ubic, C. Karthik, Experimental evidence for 'buckle, ruck and tuck' in neutron irradiated graphite, Carbon N Y. 159 (2020) 119–121. https://doi.org/10.1016/j.carbon.2019.12.028.
[21] D.K.L. Tsang, B.J. Marsden, Constitutive material model for the prediction of stresses in irradiated anisotropic graphite components, Journal of Nuclear Materials. 381 (2008) 129–136. https://doi.org/10.1016/j.jnucmat.2008.07.025.
[22] G. Haag, Properties of ATR-2E Graphite and Property Changes due to Fast Neutron Irradiation, 2005.
[23] B.T. Kelly, A.J.E. Foreman, The theory of irradiation creep in reactor graphite—The dislocation pinning-unpinning model, Carbon N Y. 12 (1974) 151–158. https://doi.org/10.1016/0008-6223(74)90021-9.
[24] C.R. Kennedy, Creep of graphite under irradiation, in: Gas-Cooled Reactor Program Semiannual Progress Report for Period Ending March 31, 1966, 198–203.
[25] A.A. Campbell, Historical experiment to measure irradiation-induced creep of graphite, Carbon N Y. 139 (2018) 279–288. https://doi.org/10.1016/j.carbon.2018.06.055.
[26] INL/EXT-17-41165, W.E. Windes, D.T. Rohrbaugh, D.W. Swank, AGC-2 Irradiated Material Properties Analysis, 2017.
[27] A.A. Campbell, G.S. Was, Proton irradiation-induced creep of ultra-fine grain graphite, Carbon N Y. 77 (2014) 993–1010. https://doi.org/10.1016/j.carbon.2014.06.016.
[28] ASTM C559-16(2020), Standard Test Method for Bulk Density by Physical Measurements of Manufactured Carbon and Graphite Articles, 2020.
[29] B.J. Marsden, M. Haverty, W. Bodel, G.N. Hall, A.N. Jones, P.M. Mummery, M. Treifi, Dimensional change, irradiation creep and thermal/mechanical property changes in nuclear graphite, International Materials Reviews. 61 (2016) 155–182. https://doi.org/10.1080/09506608.2015.1136460.
[30] G.B. Neighbour, Modelling of dimensional changes in irradiated nuclear graphites, Journal of Physics D: Applied. 33 (2000) 2966–2972.
[31] ASTM C747-16, Standard Test Method for Moduli of Elasticity and Fundamental Frequencies of Carbon and Graphite Materials by Sonic Resonance, 2020.
[32] T.D. Burchell, P.J. Pappano, J.P. Strizak, A study of the annealing behavior of neutron irradiated graphite, Carbon N Y. 49 (2011) 3–10. https://doi.org/10.1016/j.carbon.2010.08.026.
[33] ASTM C611-21, Standard Test Method for Electrical Resistivity of Manufactured Carbon and Graphite Articles at Room Temperature, 2021.
[34] H. Matsuo, Thermal annealing effects on electrical resistivity of reactor grade graphite irradiated with neutrons at 250 °C and 350 °C, Journal of Nuclear Materials. 41 (1971) 235–237. https://doi.org/10.1016/0022-3115(71)90086-9.

[35] B.T. Kelly, D. Jones, A. James, Irradiation damage to pile grade graphite at 450° C, Journal of Nuclear Materials. 7 (1962) 279–291. https://doi.org/10.1016/0022-3115(62)90245-3.
[36] A.L. Sutton, V.C. Howard, The role of porosity in the accommodation of thermal expansion in graphite, Journal of Nuclear Materials. 7 (1962) 58–71. https://doi.org/10.1016/0022-3115(62)90194-0.
[37] T.D. Burchell, W.P. Eatherly, The effects of radiation damage on the properties of GraphNOL N3M, Journal of Nuclear Materials. 179–181 (1991) 205–208. https://doi.org/10.1016/0022-3115(91)90062-C.
[38] M.C.R. Heijna, S. de Groot, J.A. Vreeling, Comparison of irradiation behaviour of HTR graphite grades, Journal of Nuclear Materials. 492 (2017) 148–156. https://doi.org/10.1016/j.jnucmat.2017.05.012.
[39] A.A. Campbell, Y. Katoh, M.A. Snead, K. Takizawa, Property changes of G347A graphite due to neutron irradiation, Carbon N Y. 109 (2016) 860–873. https://doi.org/10.1016/j.carbon.2016.08.042.
[40] L.L. Snead, T.D. Burchell, Thermal conductivity degradation of graphites due to nuetron irradiation at low temperature, Journal of Nuclear Materials. 224 (1995) 222–229. https://doi.org/10.1016/0022-3115(95)00071-2.
[41] I.I. Al-Qasir, A.A. Campbell, G. Sala, J.Y.Y. Lin, Y. Cheng, F.F. Islam, D.L. Abernathy, M.B. Stone, Vacancy-driven variations in the phonon density of states of fast neutron irradiated nuclear graphite, Carbon N Y. 168 (2020) 42–54. https://doi.org/10.1016/j.carbon.2020.05.027.
[42] S. Johns, T. Yoder, K. Chinnathambi, R. Ubic, W.E. Windes, Microstructural changes in nuclear graphite induced by thermal annealing, Mater Charact. 194 (2022) 112423. https://doi.org/10.1016/j.matchar.2022.112423.